Update to a Systematic Approach to Bearing Health Monitoring

Onder Uluyol*, Kyusung Kim*, Chris Hickenbottom**

CBM COE, Honeywell Aerospace
** 1985 Douglas Drive North Dock 1, Golden Valley, MN 55422*
*** 21111 N. 19th Ave (Deer Valley), Phoenix, AZ 85027*
Onder.Uluyol@Honeywell.com, Kyusung.Kim@Honeywell.com,
Chris.Hickenbottom@Honeywell.com

Abstract

This paper presents recent advances at Honeywell's Condition Based Maintenance Center of Excellence (CBM COE) in developing a bearing health monitoring system for a gas turbine engine. Our systematic approach characterizes bearing damage progression by identifying damage milestones based on bearing geometry. For each damage milestone, we derive appropriate condition indicators and model the damage progression as a function of these indicators. Using an oil debris monitoring (ODM) sensor, we developed a condition indicator based on particle count and size to detect the onset of a spallation while ignoring debris "fuzz." An additional condition indicator based on particle accumulation rate quantifies bursts of particles after spall initiation. A third condition indicator based on accumulated particulate mass is used throughout the failure progression and is tuned to the specific stage of damage evolution. The ODM-based condition indicators are complemented with vibration-based condition indicators. More than 300 condition indicators (CI) are defined based on vibration signals and bearing geometry. These CIs are grouped and processed hierarchically to produce second level indicators for bearing damage isolation. A two-stage fusion method, based on fuzzy logic and using ODM and vibration CIs, provides robust detection and isolation. The resulting bearing health indicators are mapped onto on-board and on-ground notices for pilots and maintainers. These notices support confirmation of impending failure by external evidence from oil filter analysis. The approach is demonstrated using rig and engine test data and scenarios describing how this approach facilitates scheduling and coordinating ground logistics are discussed.

Keywords: Bearing, Health Monitoring, Fusion, Vibration, Oil Debris

INTRODUCTION

Bearing health monitoring is one of the most critical, not yet fully developed elements of the overall vehicle health monitoring offerings. Developing a bearing health monitoring system presents two sets of challenges: 1. detection and isolation of the impending failure and 2. translating the findings into proper maintenance actions. Although any health monitoring system development faces these challenges, they are particularly difficult in

This research was partially funded by the Government under Agreement No. W911W6-07-2-003. The U.S. Government is authorized to reproduce and distribute reprints for Government purposes notwithstanding any copyright notation thereon. The views and conclusions contained in this document are those of the authors and should not be interpreted as representing the official policies, either expressed or implied, of the Aviation Applied Technology Directorate of the U.S. Government.
This document may contain information that contains material that is Copyrighted by both Bell and Honeywell.

bearing health monitoring. Detection and isolation is difficult primarily because early symptoms of impending failures are masked in the noisy environment, and the sensors are located some distance from the faulty component. Issuing maintenance actions is not straightforward, because quantitative assessment of bearing damage is difficult and untimely repair is expensive.

Electric chip detectors installed on many aircraft trigger too frequently with a high rate of No Fault Found. Weak indicators can result in aborted missions and unplanned landings, producing safety and economic consequences. Inaccurate diagnostics can reduce mission readiness and increase maintenance cost and administrative burden.

A robust bearing health monitoring system needs to offer accurate and timely detection, be able to isolate the impending failure, and provide indicators relevant for the intended user whether pilot or maintainer.

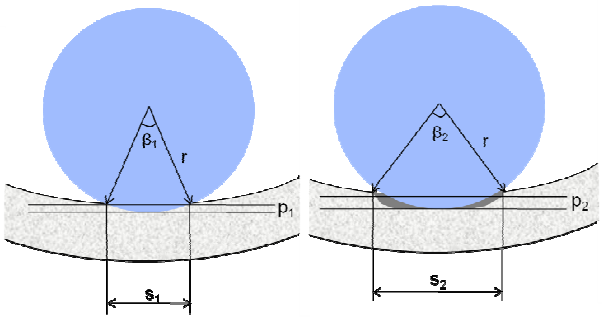
This paper presents recent advances at Honeywell's Condition Based Maintenance Center of Excellence (CBM COE) in developing an approach to realistically assess bearing condition and generate practical recommendations while considering use scenarios. In the next section, an innovative approach for characterizing bearing damage using oil debris data is presented. We then describe the process of developing ODM and vibration condition indicators and a fuzzy logic-based fusion approach. The rig and engine test setup and the algorithm validation using the experimental results are provided. Much of the contents of this paper were presented at the American Helicopter Society 66th Annual Forum [8]. Additional content discussing additional engine test reaults is included.

BEARING DAMAGE CHARACTERIZATION

Monitoring and assessing the severity of a bearing failure are difficult for several reasons. First, bearing failure is a nonlinear process and difficult to characterize. Second, the available sensors are either limited to detecting particles larger than several hundred microns or cannot provide higher resolution sensing in real time. Given these limitations, we took a practical approach. Instead of developing a continuous fault map, we identified a set of markers, called damage milestones (DM), to assess the progression of the spall growth using real-time particle detection data. We wanted to find indicators of the initiation of a spall, the transition to the rapid deterioration phase, and some markers that show the failure progression in the middle phase (propagation phase) between the initiation and the transition to the rapid deterioration points.

Detecting Spall Initiation

Though a spall may be initiated as micro pitting on the surface or as a subsurface stress concentration, the initiation stage that we are interested in detecting is a level of damage that has grown to a measurable size in terms of the debris particulate data. In addition, we sought to detect a damage level that could be a marker for further growth. We related these conditions to the given bearing geometry and estimated the spall size as shown in Figure 1a.



(a) (b)

Figure 1. (a) Initial and (b) intermediate spall damage milestones

The first damage milestone (DM_1) is characterized by a pit that has progressed to a certain depth and length. For DM_1, we set a predetermined spall depth threshold (p_1 = 75 microns). The spall length is equivalent to the arc length of the ball when the ball fits in the pit. Using the basic geometry, we can calculate the spall length at DM_1 as

$$s_1 = 2\sqrt{2rp_1 - p_1^2} \qquad (1)$$ where r is the ball radius.

Progression of Spall Severity

Upon initiation, the spall grows in the rolling direction. Using the geometry, we can measure growth in the context of the size of the bearing in question. Figure 1b shows that when the ball rotates to cover an angle β_2, the spall grows to a length s_2. For β_2 = 60 deg, a second DM can be calculated as $s_2 = \pi r/3$. Similarly for other β values, the corresponding spall lengths can be calculated using the bearing geometry.

Transition to Rapid Deterioration Phase

Spall growth during propagation can take from several to hundreds of flight hours. However, once the failure mechanism transitions into the rapid deterioration phase, we usually consider that the bearing is close to the end of its functional life. This transition is marked by an azimuth angle that spans the chord length of two adjacent balls in a bearing. It is straightforward to define a DM, marking this point as $s_3 = 2(\pi R/N + r)$ where R is the pitch radius and N is the number of balls.

Notice that the identified spall lengths depend on the specific geometry of the bearing of interest, which allows us to set meaningful thresholds on the bearing debris and facilitates better isolation.

After the initial spall damage, the spall depth does not grow beyond a certain level [1]. In our experience, this limit is about 150 microns for the kind of bearings we are interested in. The spall width is also limited by the race width, which reduces the problem to one dimension and allows us to relate the spall length at various DMs to the debris mass.

Table 1 summarizes the damage milestones and the corresponding spall length, width, and depth calculations. Table 2 shows several examples of such calculations. Notice that the amount of debris expected at various DMs cannot be expressed as a ratio of one of the DMs—in contrast to some of the applications in the industry that use an estimate similar to DM_3 and set an arbitrary percentage of it as the lower threshold.

Table 1. Damage milestones

Damage Milestone	Spall Length	Spall Width	Spall Depth
DM_1: One ball fits in initial spall depth	Compute using bearing geometry	Proportional to ball radius & spall length	75 micron
DM_2: Ball makes 60 deg rotation	Compute using bearing geometry	Proportional to race width and spall length	150 micron
DM_3: Two adjacent balls fit in spall	Compute using bearing geometry	Proportional to race width	150 micron

Table 2. Debris at damage milestones in sample bearings

Bearing No	DM_1 (mg)	DM_2 (mg)	DM_3 (mg)
Bearing #1	2.88	21.46	140.56
Bearing #2	2.11	11.59	188.04
Bearing #3	1.91	9.54	80.36

BEARING HEALTH MONITORING SYSTEM

Designing a bearing health monitoring system starts with identifying customer requirements, system requirements, and design goals in the order of priority. In this paper, we highlight several objectives that stem from these goals and reflect our practical approach.

Our first objective was to detect the incipient bearing fault as early as possible, so maintainers have sufficient time to plan before removing the engine from service. For early detection to be robust, it is critical to distinguish between false alarms and real bearing faults. Achieving this goal requires several elements. One element is to provide an initial indication when sufficient evidence shows that abnormal amounts of debris are being generated. At this point in the failure progression, the recommended action is to send the debris to a laboratory for element analysis. The maintainer can incorporate this external evidence into verifying the early failure indication.

Frequent and false indication of debris hinders the productivity. An easy, clear, and automatic method of distinguishing between normal "fuzz" and abnormal amounts of debris is needed. Our system uses criteria similar to that used by field service engineers to interpret electric chip detector indications. Unlike a chip detector, however, the bearing health monitoring system can automatically detect when the fault progresses and determine the status of the progressing fault.

Once the fault progresses to a point at which it can be annunciated with high confidence (based either on very high levels of debris or moderate levels of debris with accompanying vibration), the system will indicate to the maintainer that maintenance should be planned at the first available opportunity. This transition from unplanned to planned maintenance is valuable and another key objective of the system. If the bearing fault progresses to a level where rapid deterioration is likely before the engine is removed from service, then the pilot and the maintainer receive a final indication that immediate action is required.

Another objective of the system is to inform the maintainer of all early indications, but only inform the pilot if the fault progresses to a point that it could affect the current flight. To this end, on-board indicators can annunciate two levels of severity in flight: *use caution* and *take immediate action*. Both the on-board and the on-ground algorithms allow for updates to thresholds and other logic with minimal effort.

A secondary objective was to align isolation of the bearing fault with maintenance practices for the specific engine. The engine used to demonstrate our approach requires one of two actions if a bearing fault occurs: either open the gearbox or open the engine core. To support this maintenance approach, the algorithms isolate gearbox bearings and mainshaft bearings.

To perform the quantitative assessment of the bearing failure using DMs and align it with these objectives, the oil debris and vibration measurements are first processed to generate condition indicators (CI) and then fused together to generate health indicators (HI).

Oil Debris Monitoring CI's

An inline, full-flow inductive oil debris sensor such as the GasTops MetalSCAN sensor [2] detects particles above a minimum particle size. Extracting useful information from the raw sensor data (particle size and count) requires the data to be processed further and then mapped into CIs. One of the first steps in this process is to identify bin boundaries for particle size and monitor changes in the size distribution over time. Although the debris profile changes as the failure progresses, earlier studies have shown that CIs based on the size distribution are not robust indicators of bearing failure given the limited resolution of ODM sensors [2,3]. In addition, the relatively small number of particles detected during the initial stages of bearing failure precludes statistically robust conclusions. Given these constraints, we have found that a coarse grouping of particle size into a small, medium, and large provides more robust indicators.

We defined a composite CI that tracks the total number of medium and large particles (> 350 micron). This CI is used as a filter to detect onset of a spall by setting a count threshold below which the debris is considered "fuzz." Mathematically speaking, the count-based CI *g(x)* can be expressed as

$$g(x_c) = \begin{cases} kx_c & if\ x_c < \theta_c \\ k\theta_c & if\ x_c \geq \theta_c \end{cases} \qquad (2)$$

where x_c is the medium/large particle count, θ_c is the count threshold, and k is the particle count coefficient.

Once the medium/large particle count threshold is reached, the other CIs are activated. The next CI to be used is based on the ferrous particle mass rate. This CI is used to quantify particle bursts commonly seen in the early stages of spall progression. As shown in Figure 2, the mass rate is calculated from the detected debris amount within a given period and is mapped through a logarithmic function to produce a smooth condition indicator *h(x)*:

$$h(x_r) = \begin{cases} l\log(x_r - \theta_r + 1) & if\ x_r \geq \theta_r \\ 0 & if\ x_r < \theta_r \end{cases} \quad (3)$$

where x_r is the Fe mass rate, θ_r is the mass rate threshold, and l is the mass rate coefficient.

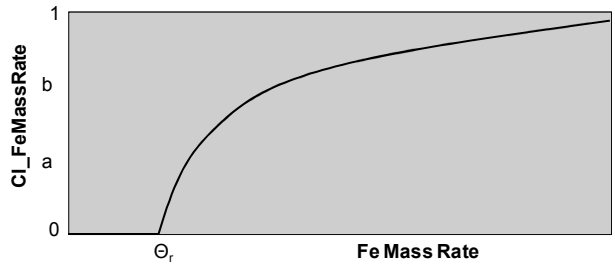


Figure 2. Fe debris mass rate mapped into CI_FeMassRate

The third condition indicator is based on the total accumulated debris mass, and it uses damage milestones, discussed above, to adjust the weighting of debris mass as shown in Figure 3.

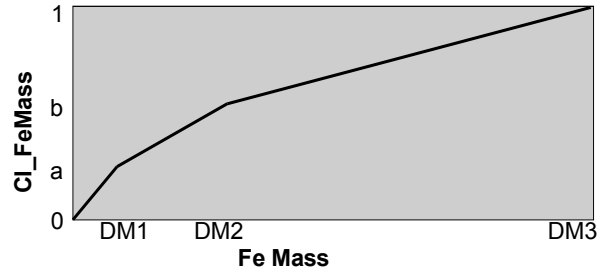


Figure 3. Mapping Fe debris mass into CI_FeMass using damage milestones

The debris mass CI, *f(x)* can be expressed as

$$f(x_m) = \begin{cases} a\dfrac{x_m}{\theta_{m,1}} & if\ x_m < \theta_{m,1} \\ (b-a)\dfrac{(x_m - \theta_{m,1})}{(\theta_{m,2} - \theta_{m,1})} + a & if\ \theta_{m,1} \leq x_m < \theta_{m,2} \\ (1-b)\dfrac{(x_m - \theta_{m,2})}{(\theta_{m,3} - \theta_{m,2})} + b & if\ \theta_{m,2} \leq x_m < \theta_{m,3} \\ 1 & if\ x_m \geq \theta_{m,3} \end{cases} \quad (4)$$

where x_m is the Fe mass, $\theta_{m,1}$ is the mass threshold based on DM_1, $\theta_{m,2}$ is the mass threshold based on DM_2, $\theta_{m,3}$ is the mass threshold based on DM_3, and a and b are the mass coefficients.

Vibration CIs

The vibration algorithm uses a combination of time and frequency domain processes to generate the condition indicators for the gear and bearing failures. The condition indicators are based on the time domain statistical properties and the spectral properties associated with the characteristic frequencies, selected harmonics, and selected side bands. The vibration algorithm runs only on certain steady-state conditions that are defined during the algorithm development stage. The algorithm monitors torque and speed at any given time

during the engine operation and determines if the current engine operating condition matches the designed vibration algorithm processing condition.

The types of vibration the CIs generated in this work are summarized in Table 3. The first six CIs (1R Peak, 2R Peak, Wide-band Bearing Energy 1, Wide-band Bearing Energy 2, Total Bearing Energy, and HF Bearing Energy) are for the bearings and are based on the vibration spectrum. The last nine CIs (Crest Factor, Energy Ratio, SLF, SI, FM0, FM4, DA1, DA2, and DA3) are for the gears and are based on the synchronous time average.

Figure 4 illustrates the vibration CIs effectiveness for detecting the fault using the data obtained in a test rig. Two CIs are shown measuring the wide-band bearing energy of the spectrum obtained from two different accelerometers—Main accel and ICP accel. The vertical line indicates the time when the fault was seeded by scoring the bearing. Both of the CIs show clear increases immediately after the fault is seeded. Note that Figure 4 shows only the very beginning of the fault initiation. The rig test continued until the bearing damage progressed; the vibration CIs showed the increases.

Figure 4 shows results from the data obtained in a test rig. On the test rig, the accelerometers are mounted close to the bearing of interest so that bearing vibrations are transmitted directly to the sensor. No other interfering signal sources drown out the signal of interest. In an engine though, the bearings are inside the engine casing. The measured vibration signals of interest are highly attenuated because they travel from the faulted bearing through the engine structure to a sensor mounted externally on the engine casing. (The sensors are mounted externally to avoid the hot operating environment and to preserve casing integrity.) The engine environment has a variety of other interfering signals such as the noise made by the combustor, the air passing through the various stages of the engine, and even from bearings and gears that will drown out the signal of interest. Thus, it is expected that the vibration CIs on a real engine will not indicate the fault as clearly in the early stages of the degradation as shown in Figure 4.

Table 3. Summary of vibration condition indicators

CI Type	CI Description	Units	Frequency
1R Peak	Magnitude of the highest single peak at the fundamental rotating speed of the shaft as defined by the tachometer	Gpk	1 per 10 min
2R Peak	Magnitude of the highest single peak at the twice of the fundamental rotating speed of the shaft as defined by the tachometer	Gpk	1 per 10 min
Wide-Band Bearing Energy 1	RMS of the frequency magnitude around the shaft fundamental rotating speed as defined by the tachometer. This CI includes the energy at the fundamental speed.	Gpk	1 per 10 min
Wide-Band Bearing Energy 2	RMS of the frequency magnitude around the shaft fundamental rotating speed as defined by the tachometer. This CI excludes the energy at the fundamental speed.	Gpk	1 per 10 min
Total Bearing Energy	RMS of the entire spectrum excluding those at the various shaft fundamental rotating speeds	Gpk	1 per 10 min
HF Bearing Energy	RMS of the spectrum at the higher frequency ranges	Gpk	1 per 10 min
Crest Factor	Synchronous average peak amp divided by RMS level	Non-dim	1 per 10 min
Energy Ratio	Std deviation of difference signal divided by std deviation of regular signal	Non-dim	1 per 10 min
SLF	Amplitude of 1R sidebands divided by std deviation	Non-dim	1 per 10 min
SI	Sum of largest Nr sidebands divided by the number of sidebands	Non-dim	1 per 10 min

FM0	Peak level of the synchronous signal average divided by the RMS average	Non-dim	1 per 10 min
FM4	Normalized Kurtosis of the signal average	Non-dim	1 per 10 min
DA1	RMS of signal average	Non-dim	1 per 10 min
DA2	RMS of residual signal	Non-dim	1 per 10 min
DA3	Peak of envelope divided by RMS of mesh	Non-dim	1 per 10 min

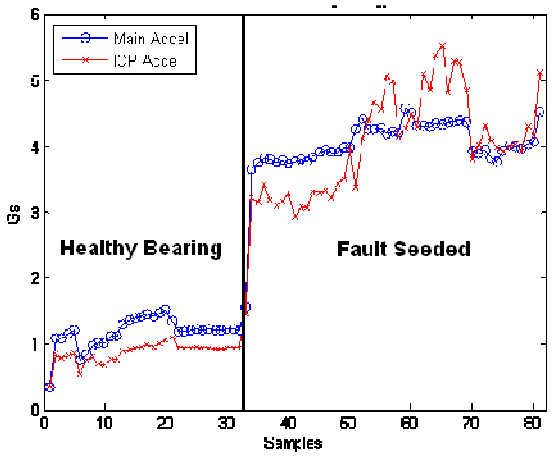


Figure 4. Bearing energy increase after scoring

By fusing the indications from the vibration and oil debris appropriately, we seek to benefit from the relative advantages of ODM and vibration CIs. The ODM provides early indication of a developing failure and compensates the issues of the vibration CIs less robust and less sensitive to the incipient faults. The vibration monitoring provides fault isolation as the fault progresses.

Two-Stage Fusion of Oil Debris and Vibration Monitoring

Information fusion from multiple indicators of damage increases the reliability of the decision, which increases true alarm rate and reduces the number of potential false alarms. The ODM gives early indication of impending failures because it can detect debris particulate and rate changes accurately, while vibration monitoring is used to diagnose the failure. This complementary use of indicators generated by two distinct technologies produces a more robust and less ambiguous overall condition indicator for engine health. It reduces the time from fault initiation to detection and supports condition-based maintenance..

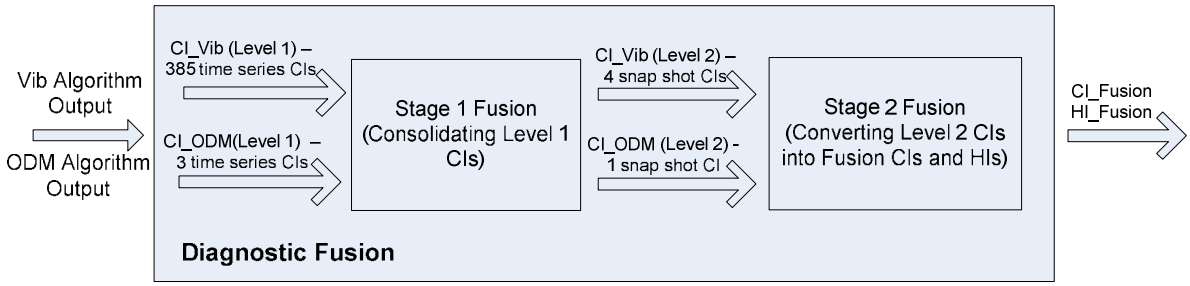


Figure 5. Two-stage fusion of the ODM and Vibration algorithms

Figure 5 shows the innovative two-stage diagnostic fusion approach developed in this work. In Stage 1 fusion, the Level 1 CIs generated from the vibration algorithm and the ODM algorithm are consolidated to generate the Level 2 CIs. The Stage 2 fusion is based on the fuzzy logic fusion and generates diagnostic health indicators and anomaly HIs. The corresponding CIs are also the output of the diagnostic fusion. The first stage evaluates all CIs to provide initial anomaly detection and groups inputs so fuzzy logic is more manageable. The second stage combines inputs from separate technologies to improve confidence in outputs.

Stage 1 ODM CI Fusion

The oil debris monitoring CIs are fused together in the first stage of the fusion module to produce an indicator called *CI_ODM_Total*. This step is expressed as

$$CI_ODM_Total = f(FeMass) + g(FeCount_ML) + u\left(\sum h(FeMassRate)\right) \quad (5)$$

where *Σh(FeMassRate)* produces the cumulative contribution of the mass rate to *CI_ODM_Total*, and the function *u(x)* limits it to the early part of the spall propagation phase by setting it to an identity function if *CI_ODM_Total* is less than 0.5 (yellow), otherwise to zero. The relative contributions of each of the ODM CIs to CI_ODM_Total changes depending on the spall growth phase. This feature is demonstrated in the experimentation section of this article using the test data.

Stage 1 Vibration CI Fusion

Some of the CIs listed in Table 3 indicate the health of a certain component, while others are more indicative of the health of the overall bearing/gear system. For example, in Table 3 we listed six types of CIs for the bearing system (1R Peak, 2R Peak, Wide-Band Bearing Energy 1, Wide-Band Bearing Energy 2, Total Bearing Energy, and HF Bearing Energy). Each bearing rotates at a different speed and the information about the health of a certain bearing is richer around its rotating speed. Among the bearing-related CIs, the first four CIs (1R Peak, 2R Peak, Wide-Band Bearing Energy 1, and Wide-Band Bearing Energy 2) extract the features from the spectrum around the narrow frequency range associated with certain rotating speeds. Thus, these four CIs are more indicative of the health of a specific bearing, which is useful for fault isolation. Since they extract the features from a very wide frequency range, the Total Bearing Energy and HF Bearing Energy CIs are used for anomaly detection.

Thus, depending on the frequency components or the synchronous time averages on which each CI is based, these CIs can be grouped according to target component. The grouping depends on the desired fault isolation level. Grouping can be at the individual bearing/gear level or it can be at a module level. The level of isolation in this work was determined by the maintenance routine in the field. The isolation at the module level is detailed enough for the maintenance practice. Thus, we group according to three module levels: core engine bearings, gearbox bearings, and gears. CIs that are not specific to these three modules, for example Total Bearing Energy and HF Bearing Energy, are grouped as 'All,' resulting in a total of four groups.

After the CIs are grouped to each target components, they are further processed to produce the CI representing each group. The processing includes normalization, since each Level 1 CI has a different scale, depending on its type and the location of the sensor on

which it is based. The processing also includes selecting which CI will represent the health condition of each target component. The CIs processed in Stage 1 fusion to represent each group is called the Level 2 vibration CI.

The demonstrator engine used in this work contains 29 bearings and 14 gears. Seven accelerometers are installed at different locations—four on the gearbox, two on the compressor, and one on the power turbine. From these seven sensors, 385 CIs are generated by the vibration algorithm. These are Level 1 CIs and the combination of the CI types defined in Table 3 by computing them from different accelerometers and different rotating speeds. Stage 1 vibration fusion produces Level 2 vibration CIs, which are four CIs representing the health condition of the engine bearings, GB bearings, gears, and the overall engine.

Stage 2 ODM and Vibration Fusion

Stage 2 fusion is the fusion of the vibration and ODM. Several approaches can be used to fuse the vibration and ODM information. In this work, the Stage 2 fusion is based on fuzzy logic [4-6] that combines evidence to construct the rules that express the health of the bearing/gear. Given the inputs of the Level 2 vibration and ODM CIs, the Stage 2 fusion generates the fusion CIs and HIs. Table 4 and Table 5 show the fusion CIs and the fusion HIs, respectively. Each CI in Table 4 has a normalized continuous value indicating the level of the damage and the anomaly. The HIs in Table 5 are the mapping of the level of the damage and the anomaly indicated by the fusion CIs into the maintenance actions represented by the color code. The mapping of the CIs into HIs is a one-to-one mapping, which means, for example, the Oil Debris Anomaly HI is a mapping of the Oil Debris Level CI and the Core Engine Bearing Health HI is mapped to the Core Engine Bearing Damage CI.

Most HIs have three color-coded states: 1) Green shows no evidence of damage or anomaly, thus no action is required; 2) Yellow shows enough damage evidence that engine removal should be scheduled; 3) Red means that the damage is severe enough that the engine will not operate reliably and should be removed immediately. The ODM Anomaly HI also produces a color code of Blue when initial evidence indicates an anomaly but not enough to recommend engine removal; thus, the maintenance action initiates filter analysis to gather corroborative evidence.

Table 4. CI_Fusion - Condition indicators generated by Fusion algorithm

CI_Fusion	Units	Frequency
Oil Debris Level	Non-dim	1 per download
Vibration Level	Non-dim	1 per download
Gearbox Bearing Damage	Non-dim	1 per download
Core Engine Bearing Damage	Non-dim	1 per download
Gear Damage	Non-dim	1 per download

Table 5. HI_Fusion – Health indicators generated by Fusion algorithm

HI_Fusion	Units	Description	Frequency
Oil Debris Anomaly	Non-dim	Green (do nothing), Blue (initiate Filter Analysis), Yellow (plan for engine removal), Red (remove engine now)	1 per download
Vibration Anomaly	Non-dim	Green (do nothing), Yellow (plan for engine removal), Red (remove	1 per download

		engine now)	
Gearbox Bearing Health	Non-dim	Green (do nothing), Yellow (plan for engine removal), Red (remove engine now)	1 per download
Core Engine Bearing Health	Non-dim	Green (do nothing), Yellow (plan for engine removal), Red (remove engine now)	1 per download
Gear Health	Non-dim	Green (do nothing), Yellow (plan for engine removal), Red (remove engine now)	1 per download

Table 6. Fuzzy system rules for ODM and vibration fusion

Rule #	IF part					THEN part	
1	Vib_EngineBearing	Low				Engine Bearing Damage	Low
2	Vib_EngineBearing	High	AND	ODM_Total	High	Engine Bearing Damage	High
3	Vib_GBBearing	Low				GearBox Bearing Damage	Low
4	Vib_GBBearing	High	AND	ODM_Total	High	GearBox Bearing Damage	High
5	Vib_Gear	Low				Gear Damage	Low
6	Vib_Gear	High	AND	ODM_Total	High	Gear Damage	High

Among the five CIs listed in Table 4, the three damage CIs (GB Bearing Damage, Engine Bearing Damage, and Gear Damage) are produced by fuzzy fusion to provide the diagnostic information needed to isolate the faults. The fault isolation is possible due to the group representation of the vibration CIs done at the Stage 1 fusion. The Oil Debris Level and Vibration Level CIs are based on the symptoms that are not isolatable to the target components; thus, they provide the anomaly indication rather than the diagnostic indication.

Implementing a fuzzy inference system requires creating fuzzy rules, designing membership functions, and selecting the fuzzy operations, implication operators, aggregation method, and de-fuzzification method. Table 6 shows the fuzzy rules for the ODM and vibration fusion, and Figure 6 and Figure 7 show the membership functions for the inputs and the outputs. For the de-fuzzification method, the mean value of the maximum (MOM) is selected.

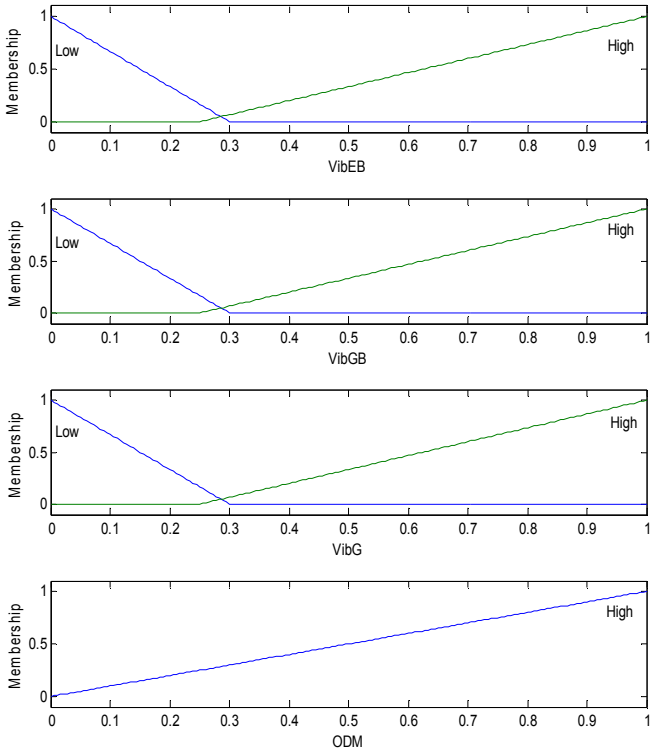


Figure 6. Fuzzy membership functions for the inputs

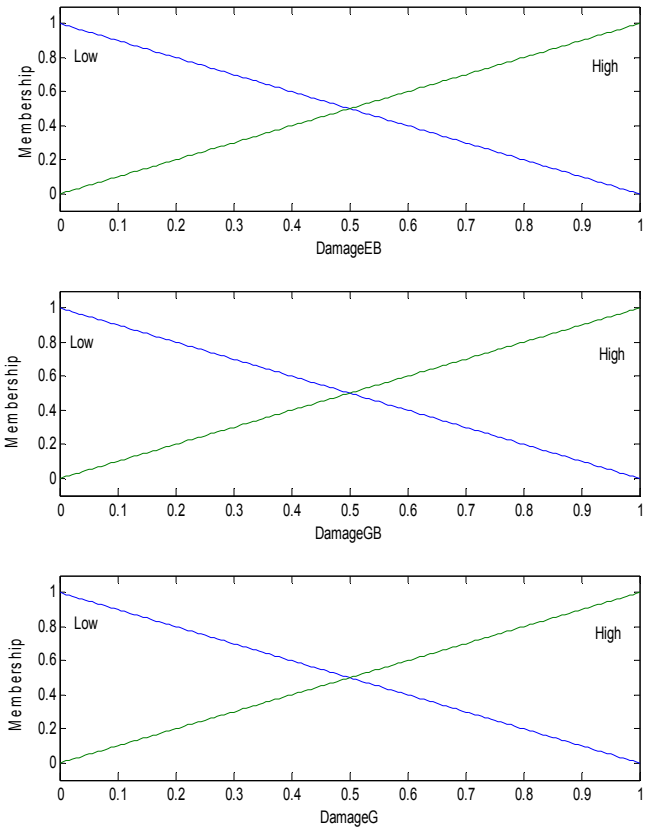


Figure 7. Fuzzy membership functions for the outputs

EXPERIMENTATION

We used seeded-fault rig and engine tests to collect data to support development of the algorithms and to demonstrate that the algorithms perform as intended. One of the challenges for seeded-fault engine tests is to make a fault develop in a manner similar the way it would develop in the field without very long run times that make the costs unacceptable. To address this challenge, we used an integrated rig/engine test approach. Faults were initiated in the test bearings and grown on the rig roughly to the point where the fault transitions from the incubation phase to the propagation phase [7]. At that point, the test bearing was removed from the rig and installed in an engine to complete the test. The engine tests consist of repeating a representative mission cycle to collect oil debris and vibration data as the fault progresses. One engine test includes a faulted engine gearbox bearing and the other engine test includes a faulted engine mainshaft bearing.



Figure 8. Engine with faulted gearbox bearing installed.

One of the first questions to answer when planning the rig tests was how to seed the fault. In general, our approach was to make an area on the inner race susceptible to a fatigue spall and then overload the bearing to initiate the spall growth. The first bearing tested had a split inner ring, which provided easy access for seeding the fault on the inner race. A Vibro-etch tool was used to lightly score the inner race, which created a stress concentration in the inner race as shown in Figure 9.



Figure 9. Bearing inner race after scoring with Vibro-Etch.

Because the inner race could not be disassembled, we needed a different seeding technique for the gearbox bearing. Here, the fault was seeded by placing a mixture of hydrochloric and phosphoric acid on the inner race. This mixture reacted with the bearing steel and created a weakness in the metal structure. After seeding the fault, the bearings were run with increasing overload until the spall began to grow. It typically took 30-60 hours for the spall to begin to grow. Figure10 shows a bearing after an extended rig test.



Figure 10. Fault progression at the end of initial rig test

Both methods for seeding the fault have advantages. The Vibro-etch method is similar to a fault caused by foreign material becoming imbedded in the bearing race. In this case, the vibration signature increases immediately after seeding the fault. The acid etch method more closely resembles a fault caused by corrosion, where the vibration signature

does not increase until bearing race material begins to shed. This method has the significant advantage of being able to seed the fault without disassembling the bearing.

Once the spall began to grow, the overload was reduced to the maximum normal load and the bearing was run at 100% speed until both vibration and ODM clearly indicated a fault. At that time, the bearing was transplanted to the engine; the oil debris data from the rig is representative of data that would have been collected if the entire test had been run in the engine. One limitation to the integrated approach is that the vibration data from the rig does not have the engine structure between the bearing and the accelerometer, nor does it have the additional noise from the other engine components.

One of the primary objectives was to determine if the bearing health monitoring system could provide a high confidence indication of an incipient fault at least 10 hours earlier than an electric chip detector can. In each test that progressed into the propagation phase of spall growth, our system provided a high confidence indication at least 28 hours before the end of the rig portion of the test. On the other hand, none of the indications from the electric chip detector during the rig tests gave a high confidence indication of a fault (based on the appropriate engine service bulletin defining how to interpret electric chip indications for that engine).

The rig tests were stopped at different points of the spall growth, typically rather early in the spall progression. In the test in which the fault was allowed to develop the furthest, the spall length at the end of the test was 0.56" as shown in Figure 10. Even though this is slightly larger than the critical threshold of 0.45" corresponding to DM_3, the bearing was still operating with acceptable race temperatures but high vibrations.

It is reasonable to assume that the bearing in this test would have continued degrading rapidly, and the electric chip detector would have provided a high confidence indication, but at that point the damage would be so severe that the bearing could no longer operate.

Another important objective of testing was to compare the information obtained from vibration, ODM, and from the fusion of the two. Here are a few observations related to this objective:

- The vibration CIs gave an immediate indication when the fault was seeded with the Vibro-etch tool. For a fault initiated by foreign debris in the bearing race, this early indication is very useful.
- The ODM CIs provide the first indication when the fault is initiated by causing material to come loose from the bearing race. In the one test where this was the case, the ODM CIs detected the fault 31 hours before the vibration CIs did.
- Beyond initial detection, both of the technologies have advantages. While the ODM CIs provide a better indication of the magnitude of the fault, the vibration CIs provide additional information to help isolate the fault.

Data Analysis

Figure 11 shows an example of a Level 2 ODM CI and the corresponding raw oil debris measurements taken during one of the tests. It is worth pointing out that while Fe debris mass and count increases as the failure progresses, the behavior generally follows a slow initial rise followed by a sharp elbow and a rapid rise.

During the initial slow rise period, it is very difficult to discern the change directly from the raw measurements. In contrast, the rise in the derived CI_ODM_Total is easily noticeable as shown by the red trajectory in Figure 11. Moreover, because of the continuous gradual rise of this indicator, the thresholds for blue (0.1 on the y-axis) and yellow (0.5 on the y-axis) indicators are crossed early on to give ample time to the maintainer to schedule engine removal.

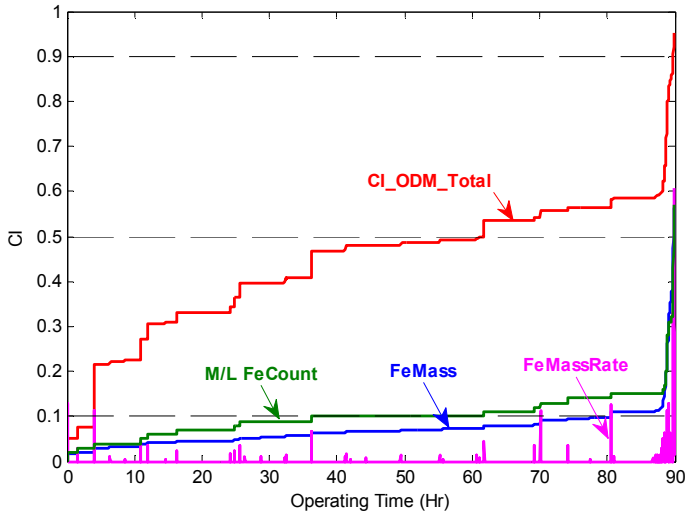


Figure 11. CI_ODM_Total vs raw ODM sensor measurements (Fe mass, Fe mass rate and the count of medium and large size Fe particles)

Figure 12 compares the same CI_ODM_Total (a Level 2 CI as shown in Figure 11) to the contribution associated with each of the Level 1 ODM CIs. As discussed above, CI_ODM_Total is a composite of CI_FeMass, CI_FeMassRate and CI_FeCount_M/L. Notice that these ODM CIs become dominant at different phases of the failure progression. CI_Fe_Count_M/L is used to detect the spall initiation and its contribution to CI_ODM_Total is limited to the early phase. Once the spall initiates, debris is produced as a burst of particles during the spall propagation. CI_FeMassRate captures and quantifies this activity, and is seen as the most dominant CI between t=5 hr to t=60 hr in Figure 12. Once the spall has grown beyond DM_2, CI_ODM_Total is determined by the accumulated Fe mass. This does not mean Fe mass is not used earlier; as discussed above, through the use of damage milestones, the weighting of Fe mass is gradually adjusted throughout the progression. Thus, the small amount of debris detected early in the spall growth has a bigger affect on CI_ODM_Total than the same amount of debris detected later.

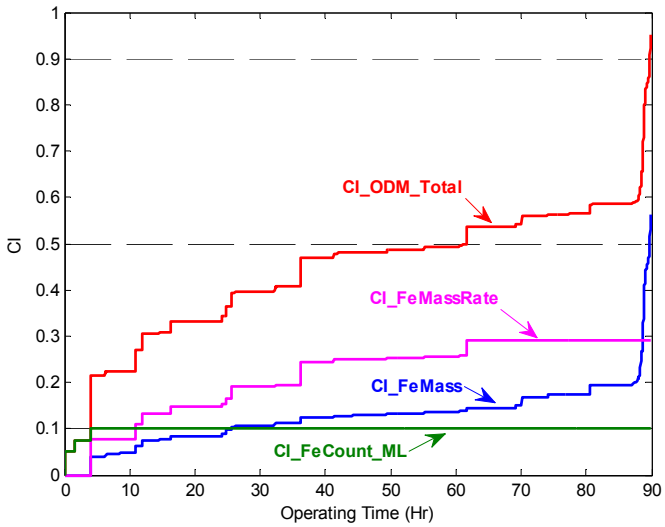


Figure 12. CI_ODM_Total vs other ODM_CIs

Figure 13 shows a sample Level 1 vibration CI and the corresponding radial load throughout the test. The first abrupt jump of bearing energy at the very beginning is right after the fault was seeded. It shows the change in vibration level upon seeding the fault. The level of the CI does not change much until it shows the second abrupt jump at the end of the rig portion of the test.

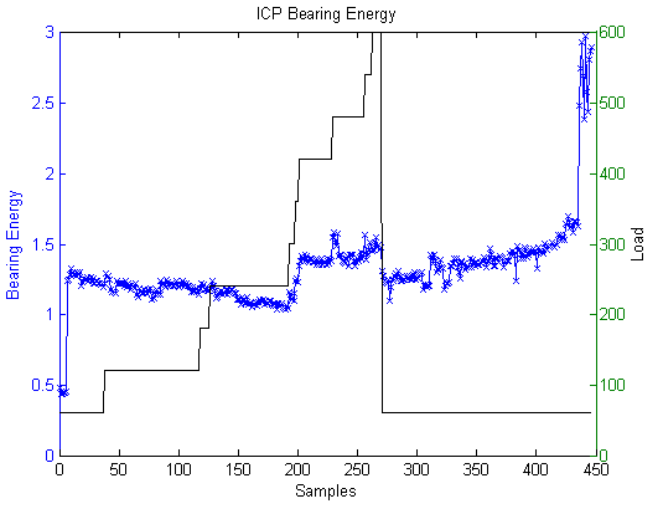


Figure 13. Level 1 vibration CI and load

Figure 14 and Figure 15 show the vibration spectrum after the fault was seeded and at the end of the test. The figures show the clear distinction of the vibration level.

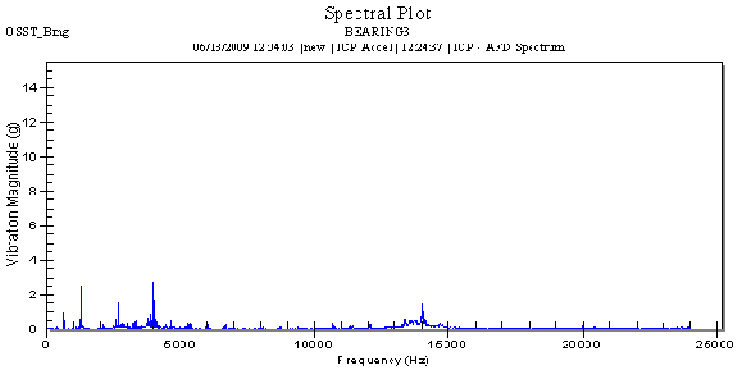


Figure 14. Vibration spectrum right after seeding a fault

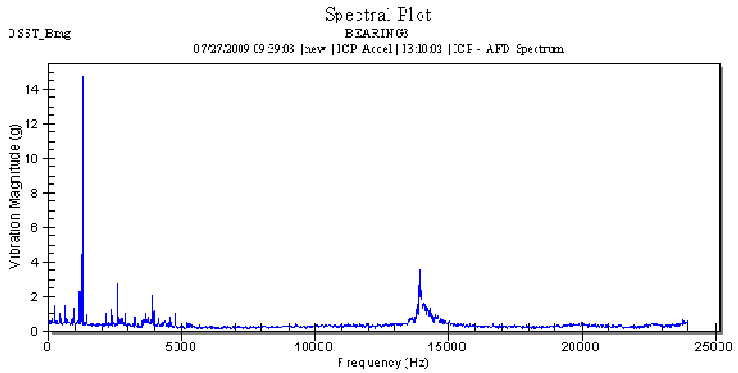


Figure 15. Vibration spectrum at end of test

Figures 16 and 17 show the overall results obtained when ODM and vibration CIs are put together using the two-stage fusion approach. A cumulative operating test time is segmented into about five-hour intervals to simulate the the way the data is downloaded from the engine at every five flight hours. Figure 16 shows the Level 2 ODM CI (labeled as ODM) and the Level 2 engine bearing vibration CI (labeled as Vibe EB). The fused CI representing the engine bearing damage (labeled as Damage EB) is computed through the fuzzy fusion of the ODM curve and the Vibe EB curve.

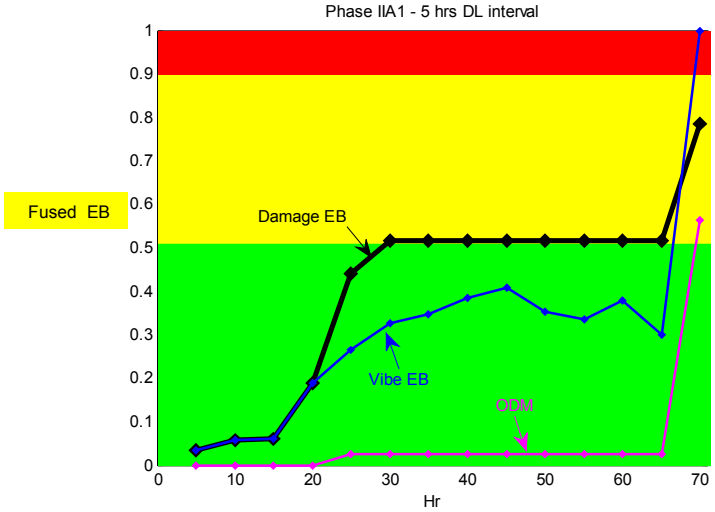


Figure 16. Fusion output in engine bearing rig test

Figure 16 shows output from the mainshaft engine bearing test. It clearly demonstrates the early indication benefit obtained from the fusion of two different indicators. Although neither the ODM CI nor the vibration CI show high activation at around 30 hrs, the fused output does exceed the yellow (0.5 on the y-axis) threshold. At the end of the test (only the rig portion is shown), both the vibration and ODM CIs rise rapidly. Thus, the fused output gives about 35 hrs of advance warning before either of the ODM or vibration CIs exceeds the yellow threshold.

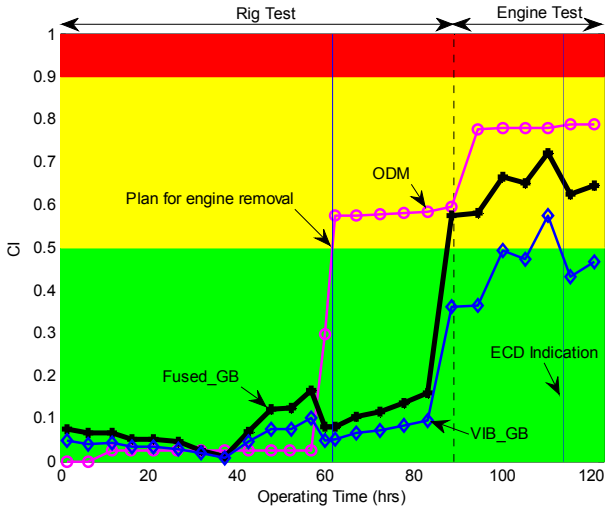


Figure 17. Fusion output in gearbox bearing tests

Figure 17 shows output from the gearbox bearing test. At around 55 hrs, the ODM starts to increase sharply and at around 60 hrs, it reaches its initial threshold of 0.1 (blue, not shown) triggering a recommendation of oil filter analysis. The ODM continues to increase and reaches yellow (0.5) after 65 hrs, recommending maintenance to plan for the engine removal. The vibration level does not increase much until around 85 hrs, and the fused CI remains in green (bottom band in figure). As the vibration CI starts to increase at around 85 hrs, the fused CI increases and reaches yellow (0.5) at 90 hrs, providing the diagnostic information. As the test continues in the engine test cell for another 30 hours, all three CIs continue to rise further. At about 27 hrs into the engine test, the first electric chip indication is seen (marked as a vertical line at t=117 hrs in Figure 17).

These results show the capability of the ODM to detect the onset of damage while the vibration level is still low. The vibration helps to isolate the fault, and the fused CI provides the diagnostic information after the damage is confirmed by the vibration CI. Note that the fused CI does not wait to go yellow until the vibration turns into yellow. It indicates yellow as soon as the vibration CI starts to increase, corroborating the damage because the ODM CI has been already at yellow.

ADDITIONAL ENGINE TESTING

In addition to the engine test with a faulted gearbox bearing, another engine test was done with a faulted mainshaft bearing. Figure 18 shows that the spall was well into the propagation phase when it was transferred from the rig to the engine.



Figure 18. Mainshaft Engine Bearing Prior to Second Engine Test

One of the primary questions to be answered during the engine tests is whether the vibration algorithms can detect the faults in the engine environment. The vibration CIs shown in Figures 19 - 20 clearly indicate a significant change when the faulted bearing was installed in the engine. The red data, labeled Phase III was collected from the baseline run with a healthy engine. The blue data, labeled Phase IV-b was collected after the faulted bearing was installed. The vibration CI shown in Figure 19 is focused on a 160 Hz window around the shaft frequency for the engine bearing, and the vibration CI shown in Figure 20 indicates a general increase in the vibration energy in the 15-21 kHz range. The figures show the increase of the CI from the beginning of the Phase IV-b test compared to the baseline at Phase III. The health condition of the bearing at the beginning of the Phase IV-b is already damaged, so the continuous progression of the vibration CI during the onset of the failure is not shown here.

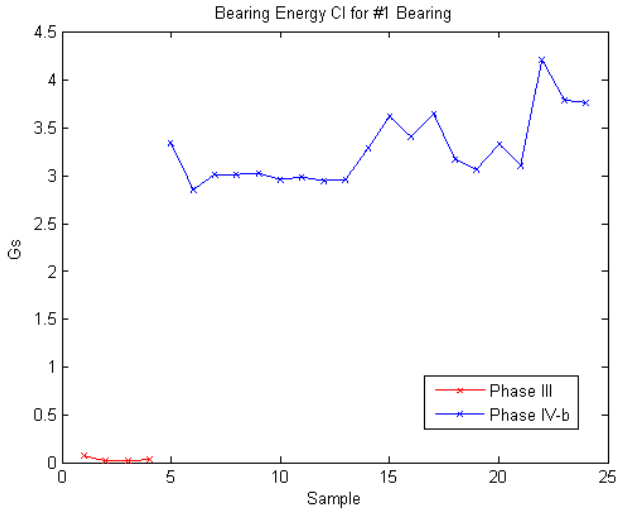


Figure 19. Change in Bearing Energy after Installing Faulted Bearing

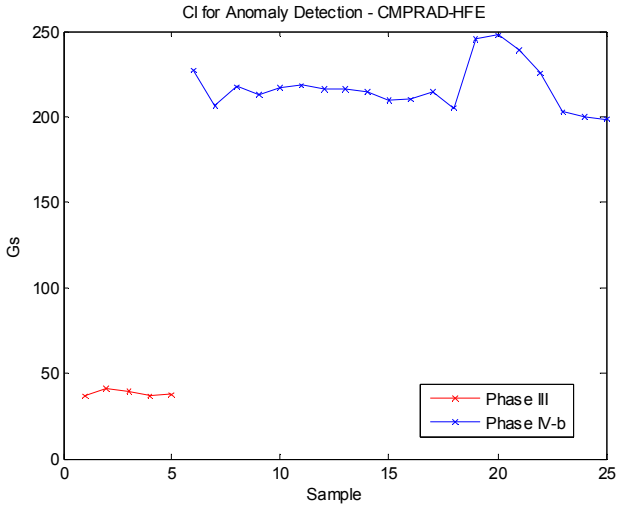


Figure 20. Change in High Frequency Energy after Installing Faulted Bearing

Figure 21 shows the overall results from the engine test with the faulted mainshaft bearing. Again, cumulative operating test time is segmented into five-hour intervals to simulate the way the data might be downloaded from the engine. The vibration CI increased immediately after scoring the bearing race, and within 20 hours reached a level that was clearly distinguishable from a healthy bearing. Note that although the vibration CI is in the red range, the system would not recommend engine removal, because the vibration indicator is primarily used to indicate normal/abnormal, rather than to indicate the severity of the fault. The first indication from ODM which was large enough to distinguish from fuzz came 25 hours after seeding the fault. This confirmation from ODM was sufficient to drive the fused CI into the yellow (high confidence) level, where the maintainer would be instructed to plan for engine removal. The first indication from the electric chip detector came 43.5 hours after the fused CI reached yellow. The second indication from the electric chip detector (which represents the high confidence indication)

came 48.8 hours after the high confidence indication from the fused CI. This well exceeds the 10 hour advanced notice target. The test was terminated shortly after the fused CI reached the red level. At that point debris was being generated rapidly, but the engine was still operating within acceptable parameters (overall vibe levels measured by the lab system were higher than normal but within limits, and bearing race temperatures were normal).

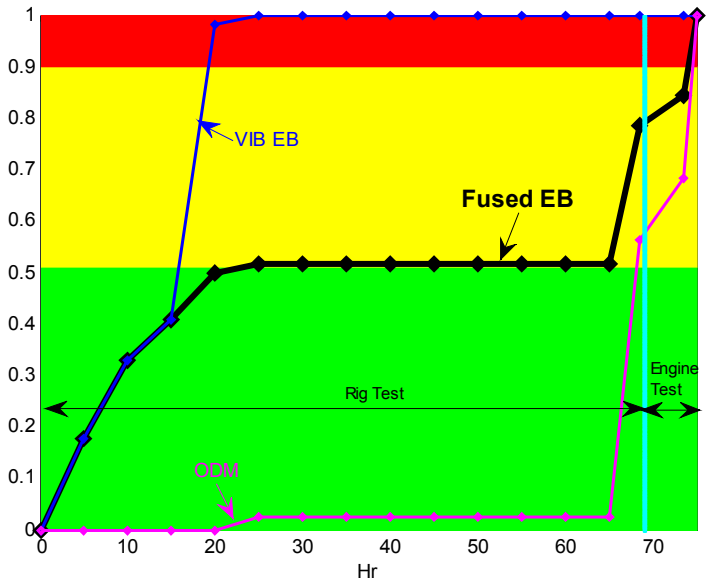


Figure 21. Fusion Output from Mainshaft Engine Bearing Tests

CONCLUSIONS

A two-stage fusion approach for detecting and isolating bearing failures has been developed at the Honeywell's recently formed Condition-Based Maintenance Center of Excellence. The approach incorporates relative advantages of oil debris and vibration monitoring in a synergistic manner.

The fusion of ODM and vibration is shown to extend the early indication window when both ODM and vibration provide some indication of the fault, but neither individual indication is at a high enough level to take action. This was particularly true in a test with the mainshaft engine bearing, where the fused output reached the high confidence threshold 35 hours before the individual CIs did.

A novel concept of damage milestones is introduced as a mechanism to monitor and assess the severity of bearing damage. The DMs are used to define weighting factors for the collected debris in order to produce a well-behaved ODM CI. Additional CIs are defined based on particle count and mass-rate. When seeding the fault by the acid method, the composite CI_ODM_Total provides an indication of bearing damage and accompanying notice for engine removal about 30 hrs in advance of the vibration indicator. In addition, CI_ODM_Total is set up to trigger an oil filter analysis, increasing the advance warning window even further. This alignment of algorithm outputs with timely maintenance activities facilitates more effective logistical support.

The two-stage fusion approach makes processing hundreds of vibration CIs manageable. By tuning vibration CIs based on rotational speed and processing them in relevant groups the failure can be isolated to the smallest maintainable unit desired.

Promising results have been obtained from the rig and engine test data for both engine and gearbox bearing failure monitoring and isolation. The approach is generic and can be implemented for different engine applications. The configuration of ODM and vibration CIs are based mainly on the bearing geometry and are easily adaptable. The fusion parameters provide the flexibility to adjust relative contributions of each to achieve advanced warning and reduced false alarms. The algorithms are designed to be implemented to provide both the on-board indications to the pilot and the on-ground notices to the maintainer.

ACKNOWLEDGEMENTS

Honeywell wishes to acknowledge that the research and development reported here was accomplished with the support and guidance of Bell Helicopter Textron, Inc.

This research was partially funded by the Government under Agreement No. W911W6-07-2-0003. The U.S. Government is authorized to reproduce and distribute reprints for Government purposes, notwithstanding any copyright notation thereon. The views and conclusions contained in this document are those of the authors and should not be interpreted as representing the official policies, either expressed or implied, of the Aviation Applied Technology Directorate or the U.S. Government.

The authors also deeply appreciate the support provided for this research by Simon Wilson of GasTOPS, and other Honeywell staff: Mark Shilo, Chris Burt, Dave Lilly, Dave Popp, Mark Diciero, and Tom Johnson.

REFERENCES

[1] Muir, D. and B. Howe, “In-Line Oil Debris Monitor (ODM) for the Advanced Tactical Fighter Engine,” Integrated Monitoring, Diagnostics and Failure Prevention. Proceedings of a Joint Conference, Mobile, AL, April 22-26, 1996.

[2] Kitaljevich, D., R. Dupuis and K. Cassidy, “Oil Debris Monitoring for Helicopter Drivetrain Condition Based Maintenance,” AHS Specialists’ Meeting on Condition Based Maintenance, Huntsville, Alabama, Feb 12, 2008.

[3] Dempsey, P.J., D.G. Lewicki, and H.J. Decker. “Investigation of Gear and Bearing Fatigue Damage Using Debris Particle Distributions,” NASA/TM—2004-212883, May 2004.

[4] Dempsey, P.J., G. Kreider, and T. Fichter. “Investigation of Tapered Roller Bearing Damage Detection Using Oil Debris Analysis,” NASA/TM—2006-214082, Feb 2006.

[5] Dempsey, P.J. and Afjeh, A.A., “Integrating oil debris and vibration gear damage detection technologies using fuzzy logic,” AHS 58th Annual Forum, Montreal, Canada, June 2002.

[6] Mendel, J.M., “Fuzzy logic systems for engineering: A tutorial,” *Proceedings of the IEEE*, vol. 83, No. 3, March 1995.

[7] Bolander, N., Qiu, H., Eklund, N., Hindle, E, and Rosenfeld, T. "Physics-based Remaining Useful Life Prediction for Aircraft Engine Bearing Prognosis," Annual Conference of the Prognostics and Health Management Society, 2009.

[8] Uluyol, O., Kim, K., and Hickenbottom, C. "A Systematic Approach to Bearing Health Monitoring," American Helicopter Society 66th Annual Forum, 2010

THE AUTHORS



Dr. Onder Uluyol is a senior scientist at Honeywell Aerospace Condition-Based Maintenance (CBM) Center of Excellence. He received his PhD in Computational Science and Engineering from the University of Illinois, Urbana-Champaign, IL. Dr. Uluyol has extensive experience in system health management and published numerous technical articles on innovative modeling, measurement, diagnostics, and control approaches. Most recently, he has been focusing on bearing health monitoring and diagnostics using oil debris and vibration monitoring. Dr. Uluyol holds six patents including one on electronic nose technology. He has six additional disclosures filed and pending.



Dr. Kyusung Kim is a senior research scientist at Honeywell Aerospace in Minneapolis, MN. His research interests are in the areas of diagnostic/prognostic information processing and decision making for performance management of valuable assets including complex dynamic systems, discrete time systems and sensors. He received his BS and MS degrees from the Seoul National University, Korea, and his PhD degree from Texas A&M University, College Station.



Chris Hickenbottom is a senior systems engineer in Honeywell Aerospace's Condition-Based Maintenance (CBM) Center of Excellence. His background is primarily with propulsion systems for Honeywell's Business and General Aviation (BGA) and Defense and Space (D&S) products. Chris has been involved in many development programs, including the AS907/HTF7000 propulsion engine, the Power and Thermal Management System (PTMS) for the Joint Strike Fighter, and the Zing™ system for the TFE731 Remote Monitoring Service. Chris received his BSME from the University of Arizona.